photon. In any event, scrambling of isotopic label in the propyl moiety is complete within the 10^{-8} s time scale of the experiment (which is defined by TOF line widths).

The reported barrier height for decomposition is 100 kJ mol^{-1} above the thermodynamic threshold.[17] The ions that live 10^{-6} s prior to decomposition in the MIKES experiment probably have energy contents only slightly greater than this barrier height. This excess energy is somewhat greater than the activation energy for hydrogen scrambling in isopropyl cation.[25] The lifetime of the ion-neutral complex, once formed, may not be substantially longer than in the photoionization/photodecomposition experiment. In the MIKES, however, the rate of scrambling is 3.7 times slower than the rate of proton transfer.

The picture that emerges, both from our simplified theoretical model and from our experiments, is that the probability of intervention of an ion-neutral complex depends upon the energy content and rotational angular momentum of the precursor parent ion. The rate of hydrogen scrambling in the alkyl moiety within the ion-neutral complex, however, is also sensitive to internal energy content. Mechanistic studies that make use of internal energy variation must weigh these considerations.

Acknowledgment. We are grateful to Professor Mostafa El Sayed of UCLA, in whose laboratories the photodecomposition experiments were performed, to Dr. Diane Szaflarski for experimental assistance, and to Professor J. L. Holmes for providing a preprint of ref 17. Ab initio calculations were performed on the Cray X-MP/48 at the San Diego Supercomputing Center. The calculations in Table I were performed by Lohri Grishow and Shari Stockwell. This work was supported by NSF Grants CHE88-02086 and CHE84-12265.

Registry No. *n*-Propyl-2,2-d_2 phenyl ether, 61809-86-7; *n*-propyl-1,1,3,3,3-d_5 phenyl ether, 123676-11-9.

(25) Koch, W.; Liu, B.; Schleyer, P. v. R. *J. Am. Chem. Soc.* **1989**, *111*, 3479-3480.

"Salted" Iron Pentacarbonyl: Molecular Isolation in Alkali Halide Solids

Ewa S. Kirkor, Donald E. David, and Josef Michl*

Contribution from the Center for Structure and Reactivity, Department of Chemistry, The University of Texas at Austin, Austin, Texas 78712-1167. *Received April 29, 1988*

Abstract: The conditions for single-molecule isolation of iron pentacarbonyl by codeposition from vapor phase onto a cold substrate with excess alkali halide vapor have been established. The photochemistry of thus "salted" $Fe(CO)_5$ has been investigated as a function of the matrix ratio. In aggregated samples, $Fe_2(CO)_9$ is formed upon irradiation. In isolated samples, three primary photoprocesses have been documented: fragmentation with a gradual loss of CO ligands, oxidation, and reduction. The latter two events are attributed to interaction with light-induced defects and color centers. Similar reactions occur spontaneously after the initial deposition, already at very low temperatures, by the interaction of $Fe(CO)_5$ with defects and color centers formed during fast quenching in the deposition process. The photochemistry of salted $Fe(CO)_5$ was compared with that of $Fe(CO)_5$ adsorbed on alkali halide films. The properties of salted CO were also investigated.

Matrix isolation of organic materials in alkali halides and other room-temperature inorganic solids has recently elicited interest.[1] These mixed materials can be prepared by vapor codeposition.

A first communication[1a] reported that many nonionic compounds can be permanently incorporated into alkali halides ("salted") by cocondensation of the corresponding vapors onto a substrate cooled by liquid nitrogen (77 K) followed by warming the deposit to room temperature and evacuating it for a time amply adequate to remove all species located on the outer surfaces. Investigation of the photochemical behavior of salted iron pentacarbonyl, 2,2-dimesitylhexamethyltrisilane, anthracene, and 1-azidoadamantane showed that the guest molecules were aggregated in the two-component systems. A three-component system consisting of $Fe(CO)_5$ in an aliphatic hydrocarbon "padding" contained an alkali halide as a rigid matrix was also described. Coincorporation of the hydrocarbon allowed room-temperature single-molecule isolation of the $Fe(CO)_5$ guest, presumably in a hydrocarbon environment.

An East German group more recently also reported a preparation of this type of material.[1b] These workers used less volatile organic dopants and codeposited them with inorganic salts onto a room-temperature substrate. They proposed the name "norganics" for the resulting organic-inorganic composites.

The present study provides full details of our results for $Fe(CO)_5$ and reports progress along two lines. First, we have now attained the goal of isolating a nonionic compound in pure alkali halide matrices at the single-molecule dispersion level. Second, we have obtained evidence for processes in which color centers and defects in the alkali halide matrices act as chemical reagents toward a nonpolar dopant isolated in the matrix and compare these with their action on substrates merely adsorbed on the alkali halide surface.

Room-temperature matrix isolation in alkali halides and other relatively inert room-temperature solids is of interest for numerous reasons. It would offer convenient room-temperature storage for reactive or volatile molecules. It would permit low-temperature and high-temperature investigation of nonpolar and polar guest molecules in a highly unusual and yet possibly quite well defined environment, which may significantly alter their spectroscopic, photochemical, and oxidation-reduction behavior. It would permit an examination of temperature-dependent properties of the isolated molecules, including the study of the equilibrium population of low-lying excited states, normally negligible at the low temperatures characteristic of ordinary matrix isolation conditions, and the study of unimolecular reactions with sizable activation barriers. It would permit the probing of defects in the solid, such as color centers, through their interaction with the dopant. In a more general sense, the effects of the doping on the properties of the host solid, such as photoconductivity, dark conductivity, absorption, and spontaneous or stimulated emission, may be of even more

(1) (a) Kirkor, E.; Gebicki, J.; Phillips, D. R.; Michl, J. *J. Am. Chem. Soc.* **1986**, *108*, 7106. (b) Bötcher, H.; Vaupel, B.; Möbius, B. *J. Inf. Rec. Mater.* **1987**, *15*, 139. Vaupel, B.; Bötcher, H. *Z. Chem.* **1988**, *28*, 253. Böttcher, H.; Hertz, O.; Fritz, T. *Chem. Phys. Lett.* **1988**, *148*, 237. Böttcher, H.; Hertz, O.; Fox, M. A. *Chem. Phys. Lett.* **1989**, *160*, 121.

0002-7863/90/1512-139$02.50/0

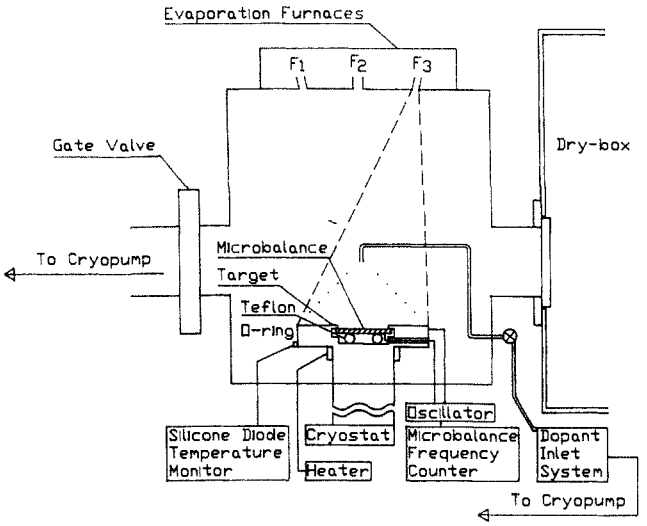

Figure 1. Ultrahigh-vacuum deposition apparatus (schematic).

interest than the effects of the host on the guest molecule.

Experimental Section

Chemicals. CsI and KBr (99.998% purity) were obtained from AESAR, $Fe(CO)_5$ from Aldrich, and spectroscopic grade methanol from Malinckrodt. Salt windows (CsI, KBr) were purchased from Harshaw. CO (99.99%) was from Spectra Gases and argon (99.998%) was from Matheson. They were used as received, except methanol, which was dried and handled under exclusion of moisture.

$CsFe(CO)_4I$ was synthesized as reported[2] at room temperature in freeze–pump–thaw degassed predried methanol either by mixing solutions of $Fe_3(CO)_{12}$ and CsI (10% excess) or by irradiation of a 5×10^{-3} M $Fe(CO)_5$ solution saturated with CsI. The thermal reaction was spontaneous. The irradiation cell was a 8-mm-i.d. quartz tube fitted with a greaseless stopcock. After the reaction, excess alkali halide was removed by cooling to −80 °C in an argon-filled glovebag and decanting while cold. Excess methanol was distilled off under vacuum, and the product was crystallized. It is stable in solution and crystalline as long as protected from air.[2] An analogous reaction of $Fe(CO)_5$ with KBr yielded $KFe(CO)_4Br$. The IR and UV spectra of $CsFe(CO)_4I$ and $KFe(CO)_4Br$ were measured in CsI and KBr pellets, respectively. Weak IR peaks appear near 1950 (w) and 2030 (m), the strongest peak lies near 1930 cm^{-1} in $Fe(CO)_4I^-$ [cf. 2018 (m), 1948 (w), and 1921 (s) reported[2] for [PPN][FeI(CO)$_4$] in THF] and it is split into a 1928- and 1932-cm^{-1} doublet in $Fe(CO)_4Br^-$.

Sample Preparation. Two types of apparatus were used for the "salting". An ultrahigh-vacuum (UHV) deposition apparatus (Figure 1) consisted of a cryopumped chamber evacuable to 2×10^{-9} Torr (Varian Cryostack 8), equipped with a set of three independent resistively heated tantalum furnaces and a gold-plated copper deposition target located 10 in. away. The target was attached to the second cooling stage of a Varian Cryostack 8 closed-cycle helium cryopump whose baffles had been removed. The target housed a quartz microbalance suitable for deposition rates of 10^{-10}–10^{-5} g/s and a 40-W heater, which permitted temperature control from 17 to 300 K. The temperatures were measured with a silicon diode at the target, a W–Rh thermocouple (W–26% Rh:W–5% Rh) at the furnace, and a J-type thermocouple at the dopant reservoir. The chamber was provided with a bakeable dopant inlet system with a Varian Model 951-5106 leak valve. The deposition temperatures were 17–23 K. All materials were transferred to and from the chamber through a nitrogen-filled drybox. The deposited samples were warmed to room temperature, evacuated to 10^{-9} Torr for at least 3 h, and placed in a protected atmosphere sample holder.

A simpler, mobile deposition apparatus was built around a Displex 202 cryostat (Air Products). The rotatable shroud was equipped with a cartridge-type evaporation furnace facing an alkali halide deposition target. In some experiments, a heat shield was introduced around the heating coil. This shielded the sample from the IR glow of the hot furnace.

A dopant inlet was located 0.5 in. in front of the furnace, facing the target. The shroud wall behind the target contained a quartz window. Rotation of the shroud by 90° brings the target into alignment with CsI windows on the remaining two shroud walls. A J-type thermocouple was used to measure the crucible temperature. The temperature of the deposition window was indicated by an Au–Fe:chromel thermocouple placed between the deposition window holder and the tip of a cryostat. For the same crucible temperature and evaporation rate, the deposition rate per unit area was 20 times higher in the Displex than in the UHV chamber, due to geometrical factors. The minimum background pressure at room temperature was in the range of 1×10^{-6} Torr, and much larger amounts of background gasses were therefore cocondensed than in the UHV chamber.

The UHV deposition apparatus was used for measuring the deposition rates of the individual components and the overall deposition rate. The rates were regulated by controlling the temperature of the salt and the dopant. It was also used for preparing samples of salted $Fe(CO)_5$ for room-temperature measurements. All other studies were performed on samples prepared in the Displex apparatus, by using deposition rates that produced single-molecule isolation as established earlier in the UHV apparatus. Thin layers of pure alkali halide were deposited on the surface at the beginning and at the end of deposition. Most of the measurements were done in situ, without removing the matrix from the deposition substrate. The fraction of $Fe(CO)_5$ retained after annealing was also measured on Displex-deposited samples prepared by using a constant salt deposition rate and various $Fe(CO)_5$ deposition rates.

Iron pentacarbonyl matrix ratios were determined by colorimetry[3] and represent total iron content in the annealed and evacuated samples.

CO diffused from the gas phase into the CsI window during deposition. Saturation was obtained by heating a 2-mm-thick CsI crystal at 200–300 °C in ~1 atm of CO overnight.

Spectral Measurements. IR spectra were recorded with 1-cm^{-1} resolution on Bomen DA 3.02 and Nicolet 60SX FTIR spectrometers equipped with a liquid nitrogen cooled MCT detector and a KBr or CsI beam splitter and calibrated with gaseous CO and H_2O. UV spectra were measured on a Cary 2300 Varian spectrometer.

In the adsorption studies of $Fe(CO)_5$ on salt surfaces, a film of pure alkali halide was deposited on the cryostat deposition window at 14 K and then exposed to $Fe(CO)_5$ vapor for 0.1–240 s. The IR spectra were measured after each exposure. $Fe(CO)_5$ pressure was controlled by keeping the reservoir temperature at 210 K and was $\sim 3 \times 10^{-2}$ Torr.[4] The reservoir was isolated from the cryostat by a Nupro NR 4JA regulating valve. The reservoir was connected with the vapor inlet port by a 4-in.-long tubing of 0.125-in. i.d. The valve was half-turn open during deposition. Samples that contained traces of water were discarded.

Photochemical Reactions. A low-pressure mercury lamp was used for all irradiations unless indicated otherwise. With the matrix thickness and doping level typically used for isolated samples, the CsI matrix absorbs most of the light at 254 nm, while KBr absorbs no more than ~20%.

Results

Isolation of $Fe(CO)_5$ in Alkali Halides. Since our ultimate objective is room-temperature matrix isolation, we consider first samples that have been deposited and brought to room temperature. Subsequently, we describe some observations concerning the initial low-temperature deposits and the annealing process. A survey of the known carbonyl stretching frequencies for a series of relevant materials is given in Table I, a survey of carbonyl stretching frequencies of decomposition products from isolated $Fe(CO)_5$ observed in our experiments is given in Table II.

(A) Annealed and Evacuated Samples. The composites of $Fe(CO)_5$ with KBr or CsI were deposited at rates below 1×10^{-7} g s^{-1} cm^{-2} on cooled substrates in the UHV chamber and freed from all evacuable components at room temperature. The removal of all volatiles leaves only guest molecules firmly embedded in the host matrix. Depending on the deposition conditions, we obtained samples whose photochemical behavior implied that $Fe(CO)_5$ is aggregated or samples whose photochemical reactivity indicated single-molecule isolation.

(a) Effect of the Matrix Ratio. The $Fe(CO)_5$ to alkali halide matrix ratio R, as determined after annealing, was varied from $R = 1{:}150$ to $R = 1{:}5000$. The actual ratios in the original deposits were higher since some $Fe(CO)_5$ is lost in the annealing process. The room-temperature annealing and evacuation procedure is essential for success in obtaining samples of consistent photochemical reactivity in the 10–300 K temperature range.

(2) Han, S.-H.; Geoffroy, G. L.; Dombek, B. D. *Inorg. Chem.* **1988**, *27*, 4355, and references therein.

(3) Brief, R. S.; Ajemian, R. S.; Confer, R. G. *Am. Ind. Hyg. Assoc. J.* **1967**, *28*, 21.

(4) Sulzmann, K. G. P. *J. Electrochem. Soc.* **1974**, *121*, 832.

Table I. CO Stretching Frequencies for Iron Carbonyls

	guest	host	T, K	$\tilde{\nu}$(FeC–O), cm^{-1}
Fe(0)	$Fe(CO)_5$	neat solid[a]	200	1948 i, w, 1956 i, w, 1977 s, 1982 s, 2003 s, 2033 m, 2115 vw
	$Fe(CO)_5$	Ar[b]	12	1998.2 s, 2003.8 s, 2006.6 m, 2008.9 s, 2023.2 s, 2025.4 s
	$Fe(CO)_5$	Si (111)[c]	90	1480–1515 w, 1650–1660 w, 2035–2065 s
	$Fe(CO)_5$	PVG[d]	RT	2004 s, 2026 s, 2114 vw
	$Fe(CO)_4Ar$	Ar[b,e]	12	1973.3 s, 1991.9 ms, 1995.8
	$Fe(CO)_4CH_4$	CH_4[e]	20	1948.9 vs, 1953 d, vs, 1981.3 d, w, 1984.2 w, 1991.0 s, 1995.6 d, s
	$Fe(CO)_4N_2$	Ar + 5% N_2[e]	20	1972 s, 1990 s
	$Fe(CO)_4$	PTFE[f]	RT	1973 s, 1992 s, 2074 w
	$Fe(CO)_4$	SiO_2[g]	150	~1940 b, ~1960 b
	$Fe(CO)_3$	Ar[e]	20	1936
	$Fe(CO)_3$	CH_4[e]		1930.4, 2040
	$Fe(CO)_2$	Ar[e]	20	1917
	Fe(CO)	Ar[h]	20	~1900
	$Na^+[HFe(CO)_4]^-$	THF[i]	RT	[1854 CO–Na^+], 1890, 1910, 2003
	$Na^+[Fe(CO)_4CN]^-$	Et_2O[i]	RT	1939 s, 1965 w, 2041 m
	$PPN^+[Fe(CO)_4I]^-$	THF[j]	RT	1921 s, 1948 w, 2018 m
	$Cs^+[Fe(CO)_4I]^-$	CsI	RT	1930 s, 1950 w, 2030 m
	$K^+[Fe(CO)_4Br]^-$	KBr	RT	1928 s, 1932 s, 1950 w, 2030 m
	$Fe(CO)_5^+$	Ar[k]	20	2116, 2124, 2127
	$Fe(CO)_5Cl^+$	BCl_4^- Nujol[l]	RT	2105 s, 2150 s, 2210 m
	$Fe(CO)_5Br^+$	BCl_4^- Nujol[l]	RT	2100 s, 2155 s, 2200 m
	$HFe(CO)_4$ O Si≡	PVG[d]	RT	2048, 2073
	cis-$Fe(CO)_4I_2$	cyclohexane[m]	RT	2060.3 s, 2083.5 vs, 2128.8 m
	trans-$Fe(CO)_4I_2$	cyclohexane[m,n]	RT	2081
	cis-$Fe(CO)_4I_2$	Ar[o]	20	2088
	cis-$Fe(CO)_4Br_2$	cyclohexane[m]	RT	2073.8 s, 2097.2 s, 2106.7 vs, 2148.5 m
	cis-$Fe(CO)_4Br_2$	Ar[o]	20	2103
	cis-$Fe(CO)_4Cl_2$	cyclohexane[m]	RT	2081.7 s, 2125.8 vs, 2166.9 m
	cis-$Fe(CO)_4Cl_2$	Ar[o]	20	2111
	$Fe(CO)_2I_2$	THF, pentane[p]	RT	2060 s, 2100 m
Fe(−1)	$Fe(CO)_4^-$	Ar[k]	20	1864.2, 1854.1
Fe(−2)	$Fe(CO)_4^{2-}$	H_2O[q]	RT	1786
polynuclear	$Fe_2(CO)_9$	neat solid[r]	200	1828 s, 2021 vs, 2063 m
	$Fe_2(CO)_9$	Ar[s]	20	1828 w, 1851 m, 1855 m, 2000 w, 2014 m, 2018 m, 2021 vw, 2024 w, 2026 w, 2032 s, 2038 vs, 2041 m, 2060 sh, 2066 vs, 2093 vw, 2111 vw
	$Fe_2(CO)_9$	N_2[s]	20	1843 w, 1847 m, 1850 m, 1998 vw, 2013 vw, 2039 vs, 2042 vs, 2062 w, 2066 vs
	$Fe_2(CO)_8$ bridged	N_2[s]	20	1821 w, 2025 s, 2033 s, 2057 s
	$Fe_2(CO)_8$ unbridged	N_2[s]	20	1973 w, 1981 w, 2008 vs, 2040 s
	$Fe_3(CO)_{12}$	Ar[t]	20	1833 ms, 1867 w, 1871 sh, 2003 vw, 2013 m, 2021 w, 2032 m, 2036 s, 2051 s, 2056 s, 2110 vw
	$Fe_2(CO)_8I_2$	THF, pentane[p]	RT	1980 s, 2000 s

[a] Reference 5. [b] Reference 10. [c] Spontaneous partial decomposition of $Fe(CO)_5$ was observed on Si (111) surface: Gluck, N. S.; Ying, Z.; Bartosch, C. E.; Ho, W. *J. Chem. Phys.* **1987**, *86*, 4957. [d] Darsillo, M. S.; Gafney, H. D.; Paquette, M. S. *J. Am. Chem. Soc.* **1987**, *109*, 3275. [e] Reference 12. [f] Reference 16. [g] Reference 15. [h] Reference 7. [i] Darensbourg, M. Y.; Barros, H. C. L. *Inorg. Chem.* **1979**, *18*, 3286. [j] Reference 2. [k] Reference 29. [l] Iqbal, Z.; Waddington, T. C. *J. Chem. Soc. A* **1968**, 2958. [m] Reference 30. [n] Noack, K. *Helv. Chim. Acta* **1962**, *45*, 1847. [o] Beattie, I. R.; McDermott, S. D.; Mathews, E. A.; Millington, K. R.; Willson, A. D. *Angew. Chem., Int. Ed. Engl.* **1988**, *27*, 1161. [p] Cotton, F. A.; Johnson, B. F. G. *Inorg. Chem.* **1967**, *6*, 2113. [q] Stammreich, H.; Kawai, K.; Tavares, Y. *J. Chem. Phys.* **1960**, *32*, 1482. [r] Reference 8. [s] Reference 13. [t] Reference 14.

Table II. CO Stretching Frequencies of the Decomposition Products of $Fe(CO)_5$ Isolated in Alkali Halide Matrices[a]

host	T, K	type[b]	$\tilde{\nu}$, cm^{-1}
KBr	298	A, I	~1900 b, ~2140 b[c]
	12	A, I	~1900 b, ~1940 sh, ~1965 sh, ~2140 b[c]
	12	B, S	1980 sh,[d] 2065 vw, 2119 w, 2139 vw,[c] 2143.5 w[c]
	20	B, I	1905 s, 1928 w, 1932 w, 2080 bw, 2105 m, ~2140 bw,[c] 2146 vw
	12	C, S	1980 wsh,[d] 2065 vw, 2119 vw, 2139 vvw, 2143.5 w[c]
	12	C, I	1906 s, 1928 vw, 1932 vw, 2070 vw, 2081 w, 2086 w, 2092 w, 2105 m, 2139 w,[c] 2144 vw
CsI	298	A, I	~1900 b, ~2140 b[c]
	298	A, J	~1900 b, ~2140 b[c]
	12	A, I	1900 w, 1940 m, 1965 s, ~2140 b[c]
	12	A, J	1900 w, 1940 m, 1965 s, ~2140 b[c]
	12	B, S	1970 sh, 2118 w, 2143 w[c]
	12	B, I	1902 m, 1926 sh w, 2081 w, 2108 w, 2137 b,[c] 2148 vw
	13	C, S	[1915, 1928 sh, 1936 sh, 1964 sh, 1980 sh, 2046 s, 2054 sh, 2120 m, 2138 sh[c]][d]
	12	D, I	1900 w, 1940 m, 1965 s, 2138 w[c]
	12	E, I	1790 vvw, 1814 vw, 1840 w, 1855,[e] 1910,[e] 1920 sh, 1940 m, 1964 s, 2015 s, 2058,[e] 2663 w, 2066 w, 2091 vvw, 2138 m[c]

[a] Irradiation products were observed at less than 10% photoconversion unless indicated otherwise: b, broad; s, strong; m, medium; w, weak; sh, shoulder; v, very. [b] A, sample annealed and evacuated at room temperature before irradiation; B, sample partially annealed by the IR glow of the salt evaporation furnace during deposition; C, sample unannealed; D, adsorbed on the surface at low coverage; E, adsorbed on the surface at high coverage; I, irradiated at 254 nm; J, irradiated at 330–350 nm; S, spontaneous decomposition. [c] Free CO. [d] Intensity poorly reproducible. [e] After extended irradiation.

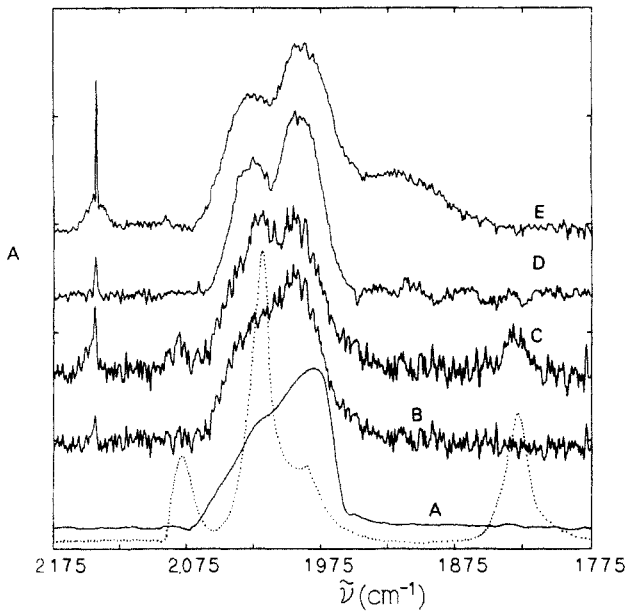

Figure 2. FT-IR spectra of $Fe(CO)_5$ (A: 12 K; B–E, 298 K). A: Solid line, neat solid; dotted line, $Fe_2(CO)_9$ produced by its irradiation. B: In KBr, matrix ratio >1:400. C: Sample B irradiated with a low-pressure Hg lamp for 10 s, photoconversion approaching 5%. D: In KBr, matrix ratio <1:1000. E: Sample D irradiated at 254 nm for 5 s, ~25% photoconversion. The $Fe(CO)_5$–KBr composites were annealed and evacuated before use.

The IR spectrum of concentrated samples, $R > \sim 1{:}400$, exhibits a broad absorption band centered at 1984 ± 2 cm^{-1} with a shoulder near 2030 cm^{-1} (Figure 2B), very similar to the IR band of frozen neat $Fe(CO)_5$[5,6] (Figure 2A). Room- or low-temperature 254-nm irradiation of these samples causes a decrease of this absorption and a concurrent appearance of three new peaks already at the lowest degrees of photoconversion. At room temperature, they occur near 1830 (m), 2020 (s), and 2080 (m) cm^{-1}. This behavior is identical with that observed in earlier work.[1a] Figure 2C shows the spectrum after a conversion of ~5%. The species responsible for the new peaks is identified as $Fe_2(CO)_9$ by comparison with the IR spectrum of an authentic sample[7,8] in CsI pellet and that of an irradiated layer of neat $Fe(CO)_5$ kept at 12 K (Figure 2A).

The UV spectra of these concentrated samples correspond to $Fe(CO)_5$ before irradiation and to $Fe_2(CO)_9$ afterward. Unlike the spectra of pure alkali halide deposits,[9] UV–visible spectra of salted $Fe(CO)_5$ ($R > 1{:}5000$), either annealed and irradiated, or unannealed, provide no evidence for the presence of ordinary color centers.

For highly dilute samples, $R < \sim 1{:}1000$, the line shape in the IR spectrum of the composite is different and two separate broad bands of $Fe(CO)_5$ are apparent in both KBr and CsI, near 1995 and 2030 cm^{-1}. This is illustrated by the room-temperature spectrum in KBr (Figure 2D) and the low-temperature spectrum in CsI (Figure 3A). For comparison we show the IR spectra of $Fe(CO)_5$ on a CsI surface at high (Figure 3B) and low coverage (Figure 3C) and in an argon matrix (Figure 3D). In argon the carbonyl stretching vibration peaks are centered at 1998–2009 cm^{-1} (assigned[7] as e′) and 2024 cm^{-1} (assigned[7] as a″) and are site-split[10] into a series of components whose bandwidth is less than 2 cm^{-1}.

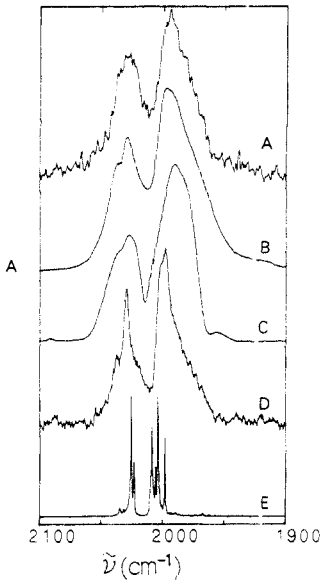

Figure 3. Matrix effects in the IR spectra of dilute ($R < 1{:}1000$) $Fe(CO)_5$ at 11–15 K. A: In CsI, annealed and evacuated at room temperature and then cooled to 12 K. B: In CsI at 12 K, annealed by the IR glow of the evaporation furnace during deposition. C: On CsI at about monolayer coverage. D: On CsI at ~1.2% of the coverage of sample C, 12 K. E: Isolated in argon.

Irradiation of the dilute samples in CsI or KBr at any temperature generates neither the IR bands of $Fe_2(CO)_9$ nor those of any other known bridging carbonyl. Instead, other IR absorption bands are produced (Figure 2E) as discussed further below.

The limiting matrix ratio at which the change from the high-concentration to the low-concentration behavior occurs is ~1:1000 in the final annealed deposit for both CsI and KBr, similar to the limiting ratio observed for isolation in rare gas matrices.[11,12]

(b) Effect of the Deposition Rate. An increase of the salt deposition rate to 1×10^{-6} g s^{-1} cm^{-2} produced samples whose room-temperature irradiation yields $Fe_2(CO)_9$ even at matrix ratio as low as 1:4000. Since the deposition rates used in earlier work were even higher, $\sim 1 \times 10^{-5}$ g s^{-1} cm^{-2}, it is not surprising in retrospect that they yielded only samples whose irradiation produced $Fe_2(CO)_9$ and were therefore deemed to be aggregated.[1a]

(c) Effect of the Deposition Temperature. This effect was studied for depositions in CsI. At low deposition rates (1×10^{-7} g s^{-1} cm^{-2}), it is possible to increase the deposition window temperature to 140 K, well above 77 K, the substrate temperature used in the unsuccessful previous attempts at molecular isolation,[1a] and still obtain $Fe(CO)_5$-containing composites whose irradiation yields no $Fe_2(CO)_9$. Samples deposited at 140–210 K contain some $Fe(CO)_5$, but lose it during the annealing and evacuation process. Those deposited above 210 K do not contain $Fe(CO)_5$. The spectra of annealed isolated samples (slow deposition, $R < 1{:}1000$) appear the same regardless of the deposition temperature.

(d) Stability of Salted $Fe(CO)_5$. The concentration of $Fe(CO)_5$ in the annealed composite remained constant when the samples were kept at room temperature under vacuum or in a drybox filled with nitrogen. Even after weeks of storage, the amount of $Fe(CO)_5$ remained the same and the irradiation produced the same products.

However, the irradiated, product-containing matrices were not stable indefinitely. At room temperature, the IR absorbance of free CO and the other product or products decayed over a period of 2 or 3 days and eventually disappeared altogether. Subsequent analysis showed that much of the iron was still present in the samples, indicating that the escaping material was probably mostly CO.

(5) Cataliotti, R.; Foffani, A.; Marchetti, L. *Inorg. Chem.* **1971**, *10*, 1594.
(6) *Comprehensive Organometallic Chemistry*; Wilkinson, Stone, Abel: Oxford, UK, 1982; Vol. 4.
(7) Geoffroy, G. L.; Wrighton, M. S. In *Organometallic Photochemistry*; Academic Press: New York, 1979.
(8) Butler, I. S.; Kishner, S.; Plowman, K. R. *J. Mol. Struct.* **1978**, *43*, 9.
(9) Tauc, J. In *Optical Properties of Solids*; Abeles, F., Ed.; North-Holland Publishing Co.: Amsterdam, London, 1972.
(10) Poliakoff, M. *Chem. Phys. Lett.* **1981**, *78*, 1.
(11) Ewing, G. E.; Pimentel, G. C. *J. Chem. Phys.* **1961**, *35*, 931.
(12) Poliakoff, M.; Turner, J. J. *J. Chem. Soc., Dalton Trans.* **1973**, 1351; **1974**, 2276; **1974**, 210.

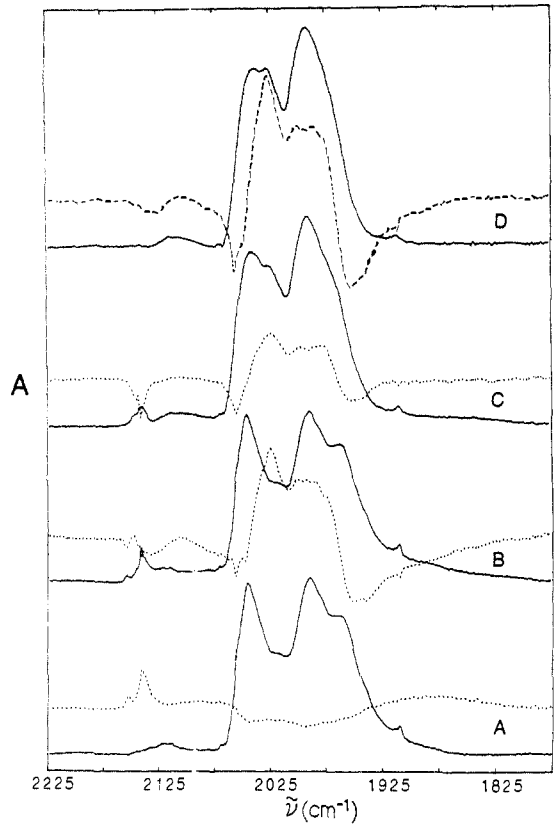

Figure 4. Effect of thermal annealing of $Fe(CO)_5$ in CsI on the IR spectrum. Solid lines: A, 13 K; B, 45 K; C, 80 K; D, 125 K. Dotted lines: difference spectra A, 45 K − 13 K; B, 80 K − 45 K; C, 125 K − 80 K. Dashed line: D, 125 K − 13 K.

(B) Unannealed Samples. Composites of $Fe(CO)_5$ with CsI were prepared in the Displex apparatus at deposition rates of 1×10^{-7} g s^{-1} cm^{-2} and final matrix ratios $R < 1{:}1000$, as measured after annealing. The samples appear glassy and transparent as long as they are kept below ~80 K. Upon warming they become opaque. This transformation is accompanied by simultaneous desorption of some of the volatile components.

The CsI–$Fe(CO)_5$ system exhibits two additional temperature ranges of major gas desorption, ~140 and ~210 K. IR spectra of the evolved gases show the presence of $Fe(CO)_5$ at all three desorption temperatures, but also the presence of CO, mainly at 80 K and less so at 140 K. Judging by IR intensities, low-concentration samples, incapable of producing $Fe_2(CO)_9$ upon low-temperature irradiation, lose less than 50% of the initially deposited $Fe(CO)_5$. More concentrated samples lose up to 95% of their $Fe(CO)_5$ load.

The spontaneous decomposition of $Fe(CO)_5$ to CO upon deposition and annealing is also evidenced by the appearance of the CO stretching band in the IR spectrum of the matrix. Its intensity relative to that of the $Fe(CO)_5$ bands was used to estimate the degree of decomposition. Samples in which this exceeded 10% were discarded. The annealing process is complex and was investigated on samples that were judged the best since they released the least gas upon annealing.

As shown in Figure 4, at ~13 K the IR bands of $Fe(CO)_5$, codeposited with a large excess of CsI on a CsI substrate at 10–20 K in the absence of IR glow from the furnace, appear at ~1990 and at ~2045 cm^{-1}, with a shoulder near 2025 cm^{-1}. The attribution of these bands is based on the results of annealing and subsequent observation of a gas-phase IR spectrum identical with that of the original $Fe(CO)_5$. In addition to the peaks of $Fe(CO)_5$, the IR spectrum exhibits weak bands attributed to decomposition products (Figure 4): a very weak and broad band of CO near 2138 cm^{-1}, a shoulder near 1965 cm^{-1}, and weak bands near 1912, 2070, and 2120 cm^{-1}.

Annealing produces complex changes. Up to 45 K (Figure 4A) one observes a spontaneous decomposition of a small part of the

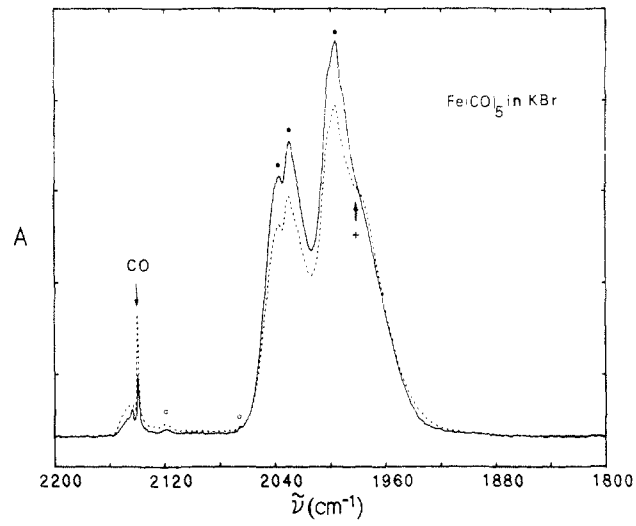

Figure 5. Spontaneous decomposition of $Fe(CO)_5$ in KBr matrix at 20 K. Solid line: IR spectrum immediately after deposition at 14 K. Dotted line: after 30 min at 20 K.

$Fe(CO)_5$ present, marked by a decrease in $Fe(CO)_5$ absorption at 1990 and 2045 cm^{-1} and appearance of (i) a very broad absorption band at ~1900 cm^{-1} and (ii) absorption bands of CO. The latter change their position and intensity several times during the annealing process (Figure 4A–C). The 1900-cm^{-1} absorption band disappears again before the temperature reaches 80 K. Above 45 K (Figure 4B–D), the bands of the remaining $Fe(CO)_5$ shift their positions to the room-temperature values of 1995 and 2030 cm^{-1}, already discussed above, presumably due to relaxation in their environment. The decomposition process is partially reversed at 80–125 K. During the reversal the bands of free CO disappear but bands of gaseous CO do not appear, although even traces would be detected readily. Apparently CO is captured by one or more of the decomposition products. The difference spectra in Figure 4 suggest that at least two decomposition products are consumed: the one absorbing at 1900 cm^{-1}, between 45 and 80 K, and the one absorbing at 1965 cm^{-1}, between 80 and 125 K. The IR bands of reconstituted $Fe(CO)_5$ initially appear near 1990 and 2025 cm^{-1} and then shift to the room-temperature values of 1995 and 2030 cm^{-1}. After all the complex changes, only these IR bands remain once room temperature is reached.

The irradiation of the substrate during deposition by the IR glow of the 1100 K furnace has a similar annealing effect on the sample (Figure 3A,B).

The behavior in KBr (Figure 5) is similar though not identical in detail and has been investigated less thoroughly. In this matrix the 13 K IR spectrum of isolated $Fe(CO)_5$ exhibits bands at 1998, 2030, and 2037 cm^{-1}. Again the sample contains peaks due to decomposition products: peaks of free CO at 2140 and 2144 cm^{-1}, a variable intensity band at 2120 cm^{-1}, and a 1980-cm^{-1} shoulder.

UV Photochemistry of $Fe(CO)_5$ Isolated in Alkali Halides. There is a significant difference in the photochemical properties of annealed and evacuated and of unannealed samples (Figure 6).

(A) Annealed and Evacuated Samples. The IR spectrum of the annealed and evacuated $Fe(CO)_5$ in CsI, recooled and irradiated at 12 K, exhibits several product bands: a broad band of CO near 2140 cm^{-1}, strong overlapping IR bands near 1970 and 1935 cm^{-1}, a very weak band near 2090 cm^{-1}, and finally one near 1900 cm^{-1}, where a band has already been observed in the annealing experiments. The last two bands are present even at low photoconversion. An analogous irradiation of $Fe(CO)_5$ in CsI or KBr at room temperature only produces the very broad absorption band at 1900 cm^{-1} and the broad band of free CO near 2140 cm^{-1} (Figure 2E).

Exhaustive UV irradiation of $Fe(CO)_5$ in CsI at 12 K destroyed all metal carbonyl IR bands and a band of free CO near 2138 cm^{-1} developed instead. The ratio of the low-temperature integrated intensities of $Fe(CO)_5$ (1900–2070 cm^{-1}) and CO

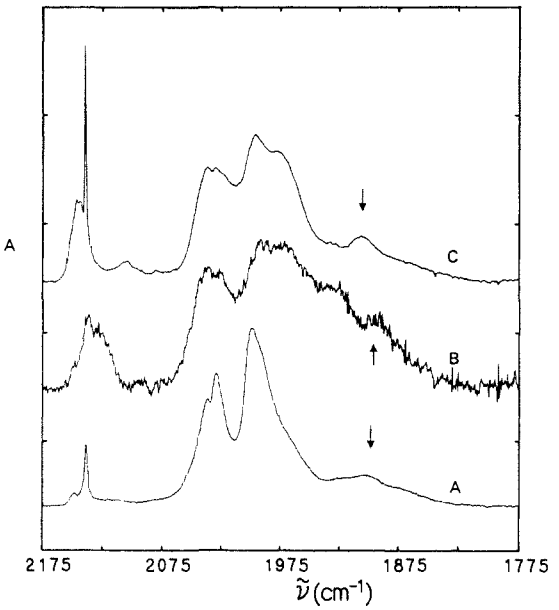

Figure 6. IR spectra of $Fe(CO)_5$ composites ($R < 1:1000$) irradiated at 254 nm at 10–20 K. A: In CsI, annealed by the IR glow of the salt evaporation furnace. B: In CsI, annealed and evacuated at room temperature before cooling for irradiation. C: In KBr, unannealed.

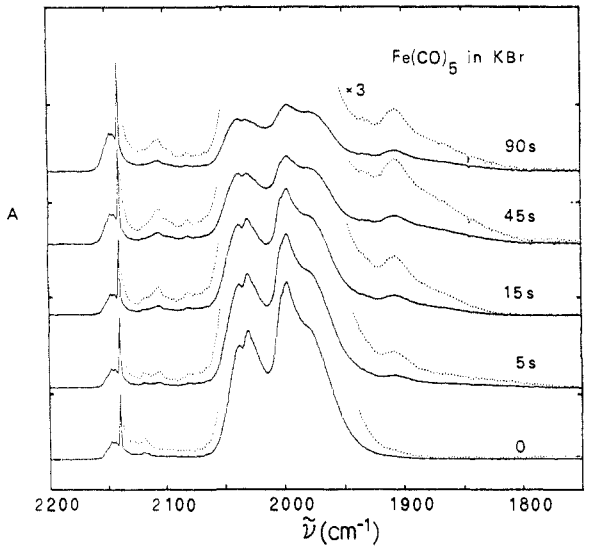

Figure 7. IR spectra of $Fe(CO)_5$ in KBr (unannealed) after consecutive 254-nm irradiations.

(2090–2175 cm^{-1}) is 29.5 ± 0.1, assuming that five CO molecules have been liberated and that $Fe(CO)_5$ is the only species initially present in the annealed matrix.

(B) Unannealed Samples. The changes in the IR spectra of irradiated $Fe(CO)_5$ in KBr are more obvious than for $Fe(CO)_5$ in CsI since there is less spectral overlap, but the basic features are identical except for minor spectral shifts. The effects of consecutive short irradiations of $Fe(CO)_5$ in KBr at 254 nm are shown in Figure 7. The initial irradiation yields at least four products: CO (2139 and 2144 cm^{-1}), a species characterized by a shoulder at 1980 cm^{-1}, another one or more with peaks at 2070, 2081, 2086, 2092, 2105, and 2120 cm^{-1} (only the last, strongest of these peaks was mentioned above), and one absorbing near 1905 cm^{-1}.

Subsequent irradiations lead to an increase of absorption of the four above products and yield another product characterized by new weak but sharp and characteristic bands at 1928 and 1931 cm^{-1}. This is identified as a small amount of $K[Fe(CO)_4Br^-]$ by comparison with the IR spectrum of an authentic sample in a KBr pellet. The last irradiation shown in Figure 7 (90 s) indicates that the 1905-cm^{-1} species is photolabile. Gradual warming of the irradiated sample (Figure 8) shows that its intensity decreases

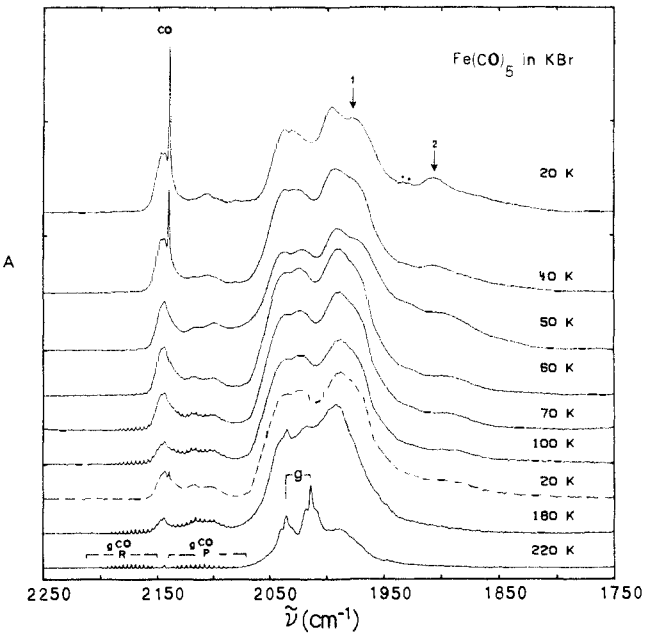

Figure 8. Top to bottom: effect of gradual warming on the IR spectrum of irradiated unannealed sample of $Fe(CO)_5$ in KBr.

upon warming, as does that of the 1980-cm^{-1} shoulder, and that $Fe(CO)_5$ is reconstituted. Release of $Fe(CO)_5$ and of the remaining CO into the gas phase is observed at higher temperatures.

At 12 K, irradiation of $Fe(CO)_5$ in CsI that has been partially annealed by the furnace glow yields the 1900-cm^{-1} species, a shoulder near 1926 cm^{-1}, CO (2148 and 2138 cm^{-1}), and a weak very broad absorption with maxima near 2066, 2081, 2108, and 2129 cm^{-1} already at very low degrees of conversion (0.1%). With the above determined ratio of $Fe(CO)_5$ and CO integrated IR absorption intensities and the assumption that the initial 1992- and 2027-cm^{-1} peaks are due solely to $Fe(CO)_5$, the rate at which they decrease relative to the rate at which the peak of free CO increases suggests that early in the irradiation, when all the light is absorbed by the matrix or by $Fe(CO)_5$, 0.93 ± 0.07 molecule of CO is produced for each $Fe(CO)_5$ molecule destroyed.

A warming of the irradiated sample in CsI to 140 K also partially reverses the photodestruction of $Fe(CO)_5$, and the bands of CO and the 1900-cm^{-1} species decrease concurrently. The set of peaks between 2066 and 2119 cm^{-1} gradually collapses into one broad band near 2097 cm^{-1} and a weak band at 1940 cm^{-1} appears. Further warming to 210 K causes the 2097-cm^{-1} band to grow and shift to 2090 cm^{-1} while $Fe(CO)_5$ and CO start escaping into the gas phase. After the sample is warmed to room temperature much weakened bands of residual $Fe(CO)_5$, CO, and the product absorbing at 1900 cm^{-1} remain.

At 140 K the proportion of products of irradiation shifts in favor of the 1965-cm^{-1} species at the expense of the 1900-cm^{-1} product and becomes similar to the result of the irradiation of a cold (12 K) annealed matrix. At 140–210 K, evolution of $Fe(CO)_5$ from the matrix during irradiation is observed. Irradiation at these temperatures yields essentially the same product bands as irradiation at 140 K, but the ratio of their intensities is poorly reproducible.

Adsorption and Photochemistry of $Fe(CO)_5$ at Polycrystalline CsI Surfaces. The IR spectra of iron pentacarbonyl adsorbed on the surface of CsI film deposited at 12 K are shown in Figure 3C,D. Three absorption bands of $Fe(CO)_5$[7] are observed, a weak one at 2091 cm^{-1} (a′) and two strong ones at 2030 (a″) and 1998 cm^{-1} (e′). The a″ and e′ vibrations are well separated at low coverage (Figure 3D). Upon increased exposure to $Fe(CO)_5$, the overlap of the bands increases (Figure 3C), the IR absorption gradually shifts to 1991 and 2028 cm^{-1} and, upon further exposure, shifts to the positions characteristic for neat frozen $Fe(CO)_5$ (Figure 2A).

At low coverage, low-temperature irradiation produces the same 1900-, 1940-, and 1965-cm^{-1} products as observed in a dilute

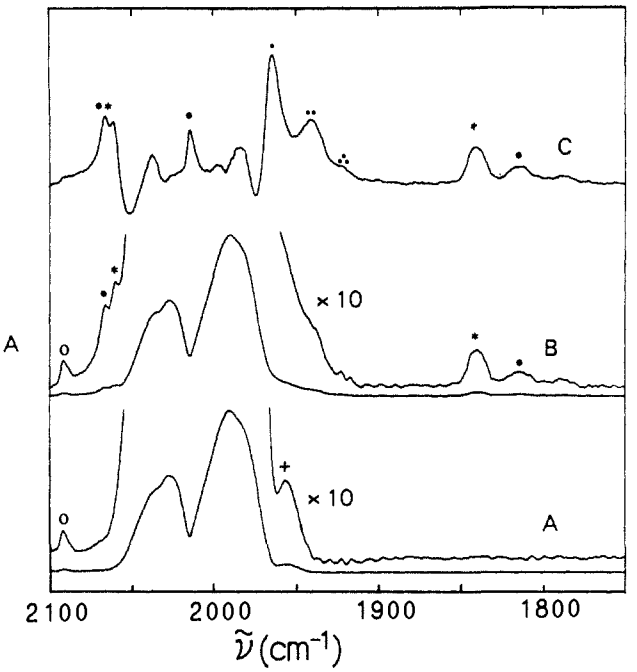

Figure 9. IR spectra of approximately one monolayer of $Fe(CO)_5$ adsorbed on a surface of CsI film at 12 K. A: Adsorbate before irradiation. The open circle marks the position of the a′ band whose intensity results from a relaxation of symmetry selection rules, the cross marks a ^{13}C satellite. B: After irradiation. The asterisks mark the bands of products, absorbing at positions characteristic for distorted $Fe_3(CO)_{12}$ and $Fe_2(CO)_9$. C: Difference spectrum B − A. Open circles: mononuclear carbonyl fragments. Asterisks: $Fe_2(CO)_9$ and $Fe_3(CO)_{12}$.

annealed and evacuated CsI matrix containing $Fe(CO)_5$. These IR bands disappear above 130 K, with liberation of gaseous CO, and stability of the photoproducts is thus markedly lower when they are merely adsorbed than when they are imbedded inside the matrix, presumably due to more facile diffusion.

At moderately high coverage sequential irradiation at low temperature yields an increasing number of product peaks (Figure 9). The stretching vibrations characteristic of bridging and terminal carbonyls of $Fe_2(CO)_9$ and $Fe_3(CO)_{12}$[8,13,14] appear at 1814, 1840, 2064, and 2066 cm^{-1}, besides the absorption bands of lower mononuclear iron carbonyls at 1920, 1940, 1941, and 1964 cm^{-1}.[6,7,15] Further irradiation produces additional new bands at 1855 and 2058 cm^{-1} that correspond to bridged carbonyls[8,13,14] and a band at 1910 cm^{-1} that possibly corresponds to $Fe(CO)_2$.[7] The $Fe_3(CO)_{12}$ is easily distorted by interaction with its environment and the vibrational bands of its bridging carbonyls shift significantly.[14] The peak at 1900 cm^{-1} characteristic for low-coverage samples is not observed now. Upon further increase in coverage the spectrum of the adsorbate becomes identical with the spectrum of neat frozen iron pentacarbonyl. As in solid iron pentacarbonyl, $Fe_2(CO)_9$ is produced upon irradiation.

The desorption of iron pentacarbonyl from a highly covered CsI film starts at 190 K. A desorption peak is observed at 210 K with a heating rate of 0.2 K/s, and the desorption is complete at 245 K.

Isolation of Carbon Monoxide in Cesium Iodide. Carbon monoxide can be incorporated in CsI at deposition temperatures up to 90 K. The IR spectrum of CO codeposited at 10–15 K recorded at deposition temperature has maxima at 2120 and 2143 cm^{-1}. A 30-s 254-nm irradiation of the matrix at 15 K completely removes both bands, apparently forcing CO out of the matrix. It is then condensed on the unirradiated surface of the cryotip and can be observed in the gas phase upon warming of the cryotip above 60 K. An increase of the sample temperature above 80 K also causes the release of CO from the matrix. The desorption of the 2143-cm^{-1} species starts before the desorption of the 2120-cm^{-1} species and is complete at 120 K. The desorption of the 2120-cm^{-1} species is complete at 160 K (Figure 10).

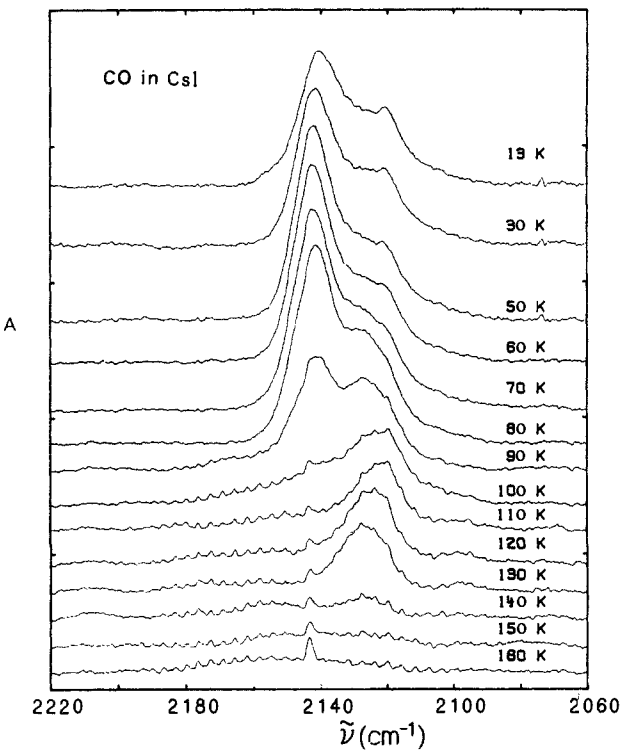

Figure 10. Carbon monoxide salted in CsI at 12 K. Top to bottom: evolution of the IR spectra upon increase of temperature from the deposition temperature (12 K) to complete loss of CO from the matrix at 180 K.

A change of the deposition temperature to 90 K affects the CO spectrum significantly. The position of the IR absorption of the deposit (broad peak at 2154 cm^{-1}) is temperature independent from 12 to 100 K. As the sample is warmed above 110 K the intensity of this peak gradually decreases and its maximum shifts to 2151.5 cm^{-1} at 160 K. At 180 K the loss of CO is complete.

Multiple layers of CO adsorbed on a CsI film absorb at 2137 cm^{-1}. The adsorbate is stable up to 60 K and desorbs at higher temperatures.

Carbon monoxide can also be incorporated in crystalline CsI by diffusion from the gas phase. The IR absorption peak occurs at 2142.5 cm^{-1} at 12 K and shifts to 2143.8 cm^{-1} upon warming to 200 K. Above this temperature, a side band appears at 2132.8 cm^{-1} (these measurements used a 0.12-cm^{-1} resolution). There is no indication that the CO incorporated in this fashion escapes from the solid upon UV irradiation, or upon extended storage at room temperature.

Discussion

Single-Molecule Isolation of $Fe(CO)_5$ in Alkali Halides. Under the conditions of single-molecule isolation, iron pentacarbonyl photochemistry in rare-gas, N_2, SF_6, or CH_4 matrices is known to proceed through a series of consecutive CO losses, leading successively to iron tetracarbonyl, tricarbonyl, dicarbonyl, monocarbonyl, and finally to a bare iron atom.[7,12] The lower iron carbonyls have also been generated by irradiation of $Fe(CO)_5$ in a polymer matrix[16] and in the gas phase.[17-19]

If allowed to anneal, matrix-isolated $Fe(CO)_4$ produces weakly bound complexes with the nearest neighbor molecule or atom of the matrix material.[12] Irradiation of partly aggregated $Fe(CO)_5$ in rare gas matrices ($R > 1{:}1000$) produces $Fe_2(CO)_9$[13] in addition to mononuclear products. This dinuclear carbonyl also is the chief

(13) Poliakoff, M.; Turner, J. J. *J. Chem. Soc. A* **1971**, 2403.
(14) Poliakoff, M.; Turner, J. J. *J. Chem. Soc. A* **1971**, 654.
(15) Jackson, R. L.; Trusheim, M. R. *J. Phys. Chem.* **1983**, *87*, 1910.
(16) De Paoli, M. A.; De Oliveira, S. M.; Baggio-Saitovich, E.; Guenzburger, D. *J. Chem. Phys.* **1984**, *80*, 730.
(17) Duncan, M. A.; Dietz, T. G.; Smalley, R. E. *Chem. Phys.* **1979**, *44*, 415.
(18) Yardley, J. T.; Gitlin, B.; Nathanson, G.; Rosan, A. M. *J. Chem. Phys.* **1981**, *74*, 370.
(19) Seder, T. A.; Ouderkirk, A. J.; Weitz, E. *J. Chem. Phys.* **1986**, *85*, 1977.

product from the room-temperature irradiation of liquid or gaseous $Fe(CO)_5$ or of its solutions and presumably arises from the addition of $Fe(CO)_4$ to $Fe(CO)_5$,[7] which appears to require little if any activation energy. It is therefore reasonable to use the formation of $Fe_2(CO)_9$ upon irradiation of $Fe(CO)_5$ as a diagnostic test for aggregation. We conclude that our samples of salted $Fe(CO)_5$ are aggregated for $R > 1:1000$ and isolated for $R < 1:1000$. The reason for our earlier failure to observe molecular isolation of $Fe(CO)_5$ in alkali halides[1a] undoubtedly was the higher deposition rate in the apparatus used at the time.

IR Absorption of Isolated Salted $Fe(CO)_5$. The IR absorption bands of $Fe(CO)_5$ isolated in KBr or CsI (Figure 6) are broad even at 14 K. They are much broader than those of $Fe(CO)_5$ isolated in solid argon or in the mixed matrix hexane–CsI.[1a] This is attributable either to a strong perturbation of the dopant by the electric field associated with the ionic charges in its immediate neighborhood or to the existence of a variety of sites available due to the large number of quite different environments generated during low-temperature deposition that remain even after annealing, or both.

Reactions of Isolated Salted $Fe(CO)_5$. The "spontaneous" decomposition and the photochemical decomposition produce similar spectral changes and apparently proceed in a similar though not identical fashion. The spontaneous damage heals completely upon annealing to room temperature, the photochemical damage does not. The well-established photochemical decomposition of $Fe(CO)_5$ and lower iron carbonyls[7,20] makes it mandatory to consider a loss of one or more CO ligands from a $Fe(CO)_5$ molecule isolated in an alkali halide as a likely primary process upon light absorption. After all, a sizeable fraction of the absorbance at 254 nm is due to $Fe(CO)_5$ in CsI matrices, and most of it is due to $Fe(CO)_5$ in KBr matrices. The exact fractions are hard to determine since an undoped "blank" matrix deposited under similar conditions absorbs even more strongly due to the presence of a much larger density of color centers. Still, there is no doubt that much of the light is absorbed by the $Fe(CO)_5$ dopant, and $Fe(CO)_4$ is a prime candidate for an initial product [recall that more concentrated samples yield $Fe_2(CO)_9$, presumably via $Fe(CO)_4$].

However, the fraction of the light that is absorbed by the matrix material can be active too, since it causes the formation of color centers,[21] which can react with $Fe(CO)_5$. The dark spontaneous decomposition must be of such an origin. The condensation of alkali halide vapor onto a cold substrate is known to create a high concentration of defects.[9,22] The relaxation of pairs of vacant cation and vacant anion lattice sites (Schottky defects) leads to the creation of pairs of color centers: the F center (excess electron) and its antimorph, V or H center (missing electron, trapped hole). The former is a reducing and the latter an oxidizing agent.

The photocatalytic properties of the surfaces of alkali halides have been attributed to the interaction of color centers with adsorbates.[23] The adsorption and desorption of simple adsorbates was previously linked to the presence of color centers in the alkali halide films,[24] and some adsorbates are known to possess specific reactivity toward electron-rich and electron-deficient centers. Thus, CO[25,26] and NO[24] form positive and negative ionic species on alkali halide surfaces and the adsorption of these gases destroys the visible coloration of the films due to the color centers.

In our composite materials similar interactions must be expected, due both to the defects generated in the initial deposition and those produced by irradiation, and in a following paper,[27] we provide evidence for the interaction of H centers with quadricyclane salted in alkali halides. Unlike the deposits of pure alkali halides, those doped with $Fe(CO)_5$ show no UV–visible absorption attributable to the usual color centers and there is little doubt that $Fe(CO)_5$ interferes with their formation, quenches them after they are formed, or both. The quenching could occur in various ways: recombination of F and H centers could be effected by their successive capture on the same iron-containing moiety in one or the other order, either (i) without a net permanent transformation of the iron carbonyl or (ii) with its thermal or electronic excitation, leading to fragmentation to a lower carbonyl and CO. The color centers could also be quenched by conversion of a fraction of an iron carbonyl to a reduced and a fraction to an oxidized product. The observed initial stoichiometry of CO appearance and $Fe(CO)_5$ disappearance suggests that such reduction and oxidation, if they play a significant role, occur with a loss of a CO ligand. Finally, it is also possible that a fraction of the originally present Schottky defects never develop into color centers and anneal with direct energy transfer to a nearby iron carbonyl molecule causing its dissociation to a lower carbonyl and CO. The thermal dissociation energy of $Fe(CO)_5$ to $Fe(CO)_4$ is only 55 kcal/mol,[28] readily available in various defect and color center transformations.

Our observations of complicated spectral changes upon gradual dark annealing of salted $Fe(CO)_5$ contained inside of or adsorbed on the surface of CsI or KBr provide evidence that one or more of these processes occur, and that the spectral simplicity of the final annealed and evacuated samples, which contain only $Fe(CO)_5$ in an alkali halide, is deceptive. Although the data are insufficient to establish the exact nature of annealing reactions, they provide clear evidence for all three general types of reactions that can be anticipated. These lead to (i) oxidation products, with the Fe atom formally in a state of positive valency, characterized by high-frequency CO stretching vibrations relative to $Fe(CO)_5$, (ii) fragmentation products, with the Fe atom still zero-valent, characterized by CO frequencies close to those of $Fe(CO)_5$ or lower, and (iii) reduction products, with the Fe atom formally in the state of negative valency, characterized by low-frequency CO stretches relative to $Fe(CO)_5$. Table I summarizes the known carbonyl stretching frequencies of the various types of likely products. At various stages of annealing, the oxidation products may regenerate V or H centers, the reduction products may regenerate F centers, and all coordinatively unsaturated products may add CO or a halide anion, offering a potential for a very complex behavior indeed. Table II summarizes the carbonyl stretching frequencies of the decomposition products from $Fe(CO)_5$ observed in our experiments under a variety of conditions. Comparison of Tables I and II suggests certain assignments, but the likely presence of potentially quite large environmental effects on the vibrations of charged species discourages a detailed discussion. Detailed assignments are perhaps best left for the future; in the following we limit ourselves to some general observations and suggestions.

(A) Oxidation Products. The products of simple one-electron oxidation of $Fe(CO)_5$ have not been well characterized in the literature. A reasonable guess would be $Fe^+(CO)_n$ plus CO.[29] However, the H centers ought to be chemically equivalent to $X_2^{\bullet-}$ and additional possible reaction products are *cis*- and/or *trans*-$Fe(CO)_4X_2$ (X = Br or I). These iron carbonyls are known to be thermally stable[30] and their IR spectra (Table I) fit well with our observed peak positions in the region 2070–2120 cm^{-1} (Table II). Since going from Fe(0) to Fe(II) requires a reaction with two H centers, perhaps unlikely at the early stages of irradiation, or a concurrent generation of an F center from an H center, perhaps also unlikely, we suspect that these peaks might be due to $Fe(CO)_4X_2^-$ instead. This hypothetical Fe(I) oxidation product ought to result from the reaction of $Fe(CO)_5$ with a single H center. The disappearance of these peaks upon warming (Figure

(20) Poliakoff, M.; Weitz, E. *Acc. Chem. Res.* **1987**, *20*, 408.
(21) Sever, B. R.; Kristianpoller, N.; Brown, F. C. *Phys. Rev. B* **1986**, *34*, 1257.
(22) Hilsh, R. In *Non-Crystalline Solids*; Frechette, V. D., Ed.; Wiley: New York, London, 1960.
(23) Ryabchuk, V. K.; Basov, L. L.; Solonitsyn, Yu. P. *React. Kinet. Catal. Lett.* **1988**, *36*, 119.
(24) Smart, St. C. *Trans. Faraday Soc.* **1971**, *67*, 1183.
(25) Rudham, R. *Trans. Faraday Soc.* **1963**, *59*, 1853.
(26) Scarano, D.; Zecchina, A. *J. Chem. Soc., Faraday Trans. I* **1986**, *82*, 3611.
(27) Kirkor, E.; Maloney, V. M.; Michl, J. *J. Am. Chem. Soc.*, following article in this issue.
(28) Engelking, P. C.; Lineberger, W. C. *J. Am. Chem. Soc.* **1979**, *101*, 5569.
(29) Breeze, P. A.; Burdett, J. K.; Turner, J. J. *Inorg. Chem.* **1981**, *20*, 3369.
(30) Johnson, B. F. G.; Lewis, J.; Robinson, P. W.; Miller, J. R. *J. Chem. Soc. A* **1968**, 867.

8) would then be due to reduction by F centers thermally released from traps.

(B) Fragmentation Products. As discussed above, these are expected to arise by loss of one and later more CO ligands. The coordinatively unsaturated lower iron carbonyls have been fairly well characterized in the IR (Table I). They do not seem to be the dominant species among our products, although the observed shoulders and peaks near 1965–1980, 1935–1940, and 1912 cm^{-1} could be associated with $Fe(CO)_4$, $Fe(CO)_3$, and $Fe(CO)_2$, respectively. However, the band we observe at $\sim$1900 cm^{-1} already appears at much too small conversions to be attributed to $Fe(CO)_2$ or Fe(CO) and more likely belongs to a reduction product. This is also suggested by the relative initial stoichiometry of the observed disappearance of $Fe(CO)_5$ and appearance of CO, which suggests an average nominal composition between $Fe(CO)_4$ and $Fe(CO)_5$ for the bulk of the primary products. However, the lower carbonyl stoichiometry is not necessarily due to free $Fe(CO)_4$.

Iron pentacarbonyl is known to react thermally or photochemically with the halogen or pseudo-halogen anions in solution to give the anions $Fe(CO)_4X^-$, presumably via $Fe(CO)_4$.[2] These anions are also formed in the gas-phase reaction of $Fe(CO)_4^-$ with halocarbons.[31] Tables I and II show that they are formed in our matrices as well. In particular, the sharp 1928-, 1932-cm^{-1} doublet in our photolyzed samples in KBr is undoubtedly due to small amounts of $Fe(CO)_4Br^-$ (Figures 7 and 8).

(C) Reduction Products. Gas-phase dissociative electron attachment to $Fe(CO)_5$ yields CO and the iron tetracarbonyl anion, $Fe(CO)_4^-$.[32] This has previously been isolated in an argon matrix.[29] Addition of an electron to $Fe(CO)_5$ in 2-methyltetrahydrofuran glass is believed to produce either $Fe(CO)_5^-$ or CO plus an unstable form of $Fe(CO)_4^-$, which transforms into a stable form upon annealing.[33] The monomeric $Fe(CO)_4^-$ anion is normally difficult to obtain since it has a pronounced tendency to add to iron carbonyl molecules.[34] It has been observed among anionic products of decomposition of iron carbonyls grafted on zeolites.[35]

Under our conditions of single-molecule isolation, $Fe(CO)_5^-$ or, $Fe(CO)_4^-$ plus CO would appear to be the likely primary products of a reaction of $Fe(CO)_5$ with an F center. The 1900-cm^{-1} frequency of our main product does not provide definitive support for either possibility, since this value differs significantly from those of $Fe(CO)_4^-$ in argon matrix (Table I), perhaps due to environmental effects, and the IR spectrum of $Fe(CO)_5^-$ appears to be unknown. The known[33,34] extreme thermal lability of $Fe(CO)_5^-$ discourages the latter assignment.

Carbon Monoxide Salted in CsI. The fact that CO introduced into a CsI matrix directly by codeposition is and CO produced within the matrix by decomposition of $Fe(CO)_5$ is not lost upon annealing and evacuation is intriguing. Even in the latter case, the CO escapes from the solid after a few days. Too little is known about detailed structure of these materials to offer a convincing explanation of this difference, or of the exact nature of the two types of sites that are distinguishable by IR spectroscopy in the CO composite deposited at 12 K. An observation of similar CO sites was reported in an investigation of CO adsorbed on a low-temperature film of vapor-deposited KCl.[26]

The site in which CO resides in matrices prepared by deposition at 90 K is different from either of the two populated during deposition at low temperature. Since CO adsorbed on a KCl film has a tendency to reorganize into stable islands of σ-physisorbed CO,[36] we propose that a similar aggregation process takes place during deposition on a support at 90 K. It is noteworthy that CO can be deposited in CsI at 90 K at all, considering that it escapes from lower temperature deposits already upon warming to 80 K. Perhaps the larger aggregates are localized in relatively stable caverns ("salt domes") while the isolated CO is substitutional, occupying a Schottky defect (a missing CsI ion pair), and much more mobile. The rapid elimination of isolated CO from the CsI matrix by UV irradiation at 15 K is probably due to association of the CO with photogenerated color centers into a more mobile defect.

The isolated CO molecules definitely occupy sites different from those taken by CO that has diffused into a crystal of CsI from the gas phase, presumably into interstitial positions. The latter absorbs at 2143.8 and 2132.8 cm^{-1} and appears to be insensitive to UV irradiation.

Thus, we find it likely that the 2120- and 2143-cm^{-1} sites in the low-temperature deposits correspond to CO isolated in a Schottky defect, while the 2154-cm^{-1} site in the high-temperature deposit corresponds to aggregated CO in a larger cavern, and the 2143.8- and 2132.8-cm^{-1} sites populated by diffusion correspond to interstitial CO.

Summary

Suitable conditions for the single-molecule isolation of iron pentacarbonyl and probably also carbon monoxide inside alkali halide microcrystals have been found. We expect them to provide access to similar permanent salting of many other organic and inorganic nonpolar molecules. Two such examples, quadricyclane and norbornadiene, are studied in the following paper.[27] It appears likely that the technique can be extended not only to other guests but also to other hosts that are solid at room temperature but form high-temperature vapors.

Investigations of the annealing and photochemical behavior of these novel materials suggest a strong involvement of lattice defects and color centers in chemical processes involving the dopant, and alkali halide lattices can be thought of as distinct chemical environments. Their reactivity makes them quite different from the more usual low-temperature matrix materials, the noble gases.

The properties of our matrices complement those of other solids and glasses that have been used for solute isolation and immobilization at or near room temperature. Most of these are organic (polymers, adamantane), some are inorganic (boric acid, zeolites, and recently,[37] doped silica glass). The disadvantages of alkali halides as room-temperature matrices are poor optical quality in the UV and visible regions due to microcrystallinity and the limitation to at least somewhat volatile dopants. Their advantages are transparency in the IR region, high rigidity, and absence of abstractable hydrogens and reactive hydroxyl groups. The strong electric fields present (Madelung potential) and the availability of oxidation–reduction agents in the form of color centers may represent an advantage or a disadvantage, depending of the intended application, and make these materials particularly interesting. Finally, it is to be noted that less volatile dopants permit deposition at higher temperatures and yield composites of good optical quality even in the visible region.[1b]

Acknowledgment. This project was supported by the U.S. Army Research Office (Contract DAAL 03-87-K-0055).

Registry No. $Fe(CO)_5$, 13463-40-6; $CsFe(CO)_4I$, 123835-14-3; $KFe(CO)_4Br$, 123835-15-4; CO, 630-08-0; CsI, 7789-17-5; KBr, 7758-02-3.

(31) McDonald, R. N.; Schell, P. L.; McGhee, W. D. *Organometallics* **1984**, *2*, 182, and references therein.
(32) Compton, R. N.; Stockdale, J. A. D. *Int. J. Mass. Spectrom. Ion Phys.* **1976**, *22*, 47.
(33) Peake, B. M.; Symons, M. C. R.; Wyatt, J. L. *J. Chem. Soc., Dalton Trans.* **1983**, 1171.
(34) Krusic, P. J.; San Filippo, J.; Hutchinson, B.; Hance, R. L.; Daniels, L. M. *J. Am. Chem. Soc.* **1981**, *103*, 2129.
(35) Iwamoto, M.; Nakamura, S.-I.; Kusano, H.; Kagawa, S. *J. Inclusion Phenom.* **1986**, *4*, 99.
(36) Heidberg, J.; Stein, H.; Hussla, I. *Surf. Sci.* **1985**, *162*, 470.
(37) For leading references, see: Levy, O.; Avnir, D. *J. Phys. Chem.* **1988**, *92*, 4734. Kaufman, V. R.; Avnir, D.; Pines-Rojanski, D.; Huppert, D. *J. Non-Cryst. Solids* **1988**, *99*, 379.